Rare Metal Materials and Engineering
Volume 48, Issue 12, December 2019
Available online at www.rmme.ac.cn

Science Press

Cite this article as: Rare Metal Materials and Engineering, 2019, 48(12): 3806-3811.

ARTICLE

Effect of Microscopic Stress and Strain on Mechanical Properties of Ti-6Al-2Zr-1Mo-1V Alloy

Ji Zhe, Guo Tao, Shen Chengjin, Xu Jie

China University of Mining and Technology, Xuzhou 221116, China

Abstract: Analysis of the effect of constituent phases on mechanical properties is critical to the design of microstructure of titanium alloys. For this reason, the microscopic stress and strain in soft primary α (α_p) and hard transformed β matrix (β_t) were quantitatively analyzed by a microstructure-based finite element model to determine their effect on strength and ductility of Ti-6Al-2Zr-1Mo-1V alloy. The results show that microscopic stress in both α_p and β_t shows a normal distribution. The peak stress and stress peak height of β_t are much larger than those of α_p. While, α_p has large peak strain and β_t has large strain peak height. As α_p volume fraction decreases from 49% to 12%, the contribution of β_t to ultimate tensile strength (UTS) and failure strain (FS) of the alloy increases from 59% to 91% and 36% to 75%, respectively. However, as the contribution of β_t increases, UTS of the alloy increases by 17% and FS decreases by 21%. This finding quantitatively reveals the effect of constituent phases on strength and ductility and provides a basis to the design of microstructure of titanium alloys.

Key words: microscopic stress and strain; constituent phases; mechanical properties; titanium alloys; finite element simulation

Titanium alloys are often used to produce key bearing components in aviation and aerospace industries due to their excellent mechanical properties[1,2]. Microstructural design is an effective way to obtain high performance titanium alloys, since size, volume fraction, morphology and mechanical property of each constituent phase in the alloys can be changed significantly through various thermomechanical processing[3,4]. However, during deformation of titanium alloy, the constituent phases interact with each other in a complicated manner due to their complex and diverse parameters, which makes it difficult to determine the contribution of each constituent phase to the overall properties and to design the microstructure of titanium alloys. Microscopic stress and strain are the comprehensive response of the deformation and interaction of various constituent phases, which determine the mechanical properties of titanium alloys[5]. Therefore, quantitative analysis of microscopic stress and strain is an effective way to determine the contribution of each constituent phase to the properties of titanium alloys.

By now, many efforts have been devoted to investigate the microscopic strain in titanium alloys by experimental methods. In-situ X-ray diffraction[6] and neutron diffraction[7,8] experiments show that significant strain partitioning is formed between α and β phases during deformation of titanium alloys. However, these methods have no information about strain distribution. Microscopic strain is considered to be unevenly distributed in each phase, which has a significant effect on the ductility of materials[9]. Digital image correlation technique[10] and sampling moiré method[11] reveal that microscopic deformation heterogeneity is established early in the plastic regime and damage formation site and final failure of Ti-6Al-4V are controlled by the microstructural strain localization.

Recently, a microstructure-based finite element approach is used to investigate the microscopic deformation of material[12,13]. It is found that soft primary α (α_p) phase tends to concentrate plastic strain and stress will be localized in hard transformed β matrix (β_t) and stress gradients exist in both α and β phases[14,15]. The microstructure-based finite element models also show that microscopic stress and strain localization occurs due to incompatible deformation between

Received date: December 20, 2018
Foundation item: Fundamental Research Funds for the Central Universities of China (2015QNA04)
Corresponding author: Ji Zhe, Ph. D., School of Materials Science and Engineering, China University of Mining and Technology, Xuzhou 221116, P. R. China, Tel: 0086-516-83591879, E-mail: jizhe@cumt.edu.cn

Copyright © 2019, Northwest Institute for Nonferrous Metal Research. Published by Science Press. All rights reserved.

α_p and β_t which can be modified by tailoring microstructural parameters. Fine α particles may induce more homogeneous deformation in β phase than coarse α particles[16]. The degree of strain localization will be decreased by decreasing the disparity of strength between α_p and β_t[17] or changing the morphologies of α from lamellar to equiaxed[18].

In this paper, based on the scanning electron micrograph (SEM), a real microstructure-based finite element model for Ti-6Al-2Zr-1Mo-1V (TA15) alloy was developed to investigate the microscopic stress and strain in α_p and β_t during deformation. Both the microscopic stress and strain were characterized quantitatively and their relative contributions to the properties of TA15 alloy were studied. It will deepen the understanding of the effect of microstructure on properties and provide a basis for microstructural design of the titanium alloys.

1 Microstructure-based Finite Element Modeling

In order to investigate the microscopic stress and strain in constituent phases with different parameters, the microstructures of TA15 samples were changed using different heat treatment routes (S12, S22, and S49), as listed in Table 1. The microstructures observed by VEGA TESCAN scanning electron microscope are shown in Fig.1. As shown in Fig.1, the microstructures contain equiaxed α_p particles embedded in β_t matrix. The size and volume fraction ($V_{\alpha p}$) of α_p increase with decreasing first heat treatment temperatures (listed in Table 1). Two different thicknesses of α plates within β_t which are secondary and tertiary α[19] are obtained after the heat treatments. The thickness variation of α plates will change the hardness of β_t.

The microstructures in Fig.1 are used to develop the representative volume elements (RVE) of the microstructure-based finite element models. The modeling procedure is shown in Fig.2. The SEM image is first binarized to distinguish α_p and β_t. The boundary lines of α_p are converted from raster to vector form and then input into Abaqus to define the geometry structure of the RVE. Two-dimensional plane stress elements, CPS3, are used to simulate the uniaxial tension of the TA15 alloy sheet samples. Periodic boundary conditions are applied on the boundary of RVE. The constitutive model of β_t is determined by reversely analyzing indentation load-depth curves and the constitutive model of α_p is obtained by analyzing its strengthening mechanism[17]. In the simulation, α_p and β_t are treated as two distinct microstructural units and the boundary between them is assumed to be perfect bonding. After simulation, the microscopic stress and strain in constituent phases can be obtained directly and the stress-strain curve of the alloy is obtained by homogenization method.

The predicted and experimental stress-strain curves of the uniaxial tension of the TA15 alloy samples are shown in Fig.3. As shown in Fig.3, the predicted results are in good agreement with the experimental results. So, it can be concluded that the developed models have the intrinsic ability to capture mechanical response of the alloy. The predicted ultimate tensile strength (UTS) and failure strain (FS) of TA15 titanium alloy samples are shown in Table 1. The UTS increases from 941 MPa to 1098 MPa and the FS decreases from 15.8% to 12.5% with decreasing the volume fraction of α_p. It should be noted that FS is predicted using the plastic strain localization theory[13]. This theory predicts the ductile failure as a natural outcome of plastic strain localization induced by microstructure-level inhomogeneity and has well predicted the failure of titanium alloys[20] and other alloys[21].

2 Results and Discussion

2.1 Microscopic stress distribution

With the microstructure-based finite element model established, the microscopic stress and strain in α_p and β_t during

Table 1 Heat treatment routes of TA15 alloy samples and corresponding microstructure and property parameters

Samples	Processing routes	Size/μm	$V_{\alpha p}$/%	UTS/MPa	FS/%
S12	975 °C/20 min/AC +950 °C/20 min/WQ	11.34	12	1098	12.5
S22	965 °C/20 min/AC +940 °C/20 min/WQ	12.32	22	1040	14.8
S49	910 °C/20 min/AC +885 °C/20 min/WQ	14.36	49	941	15.8

AC-air cooling; WQ-water quenching

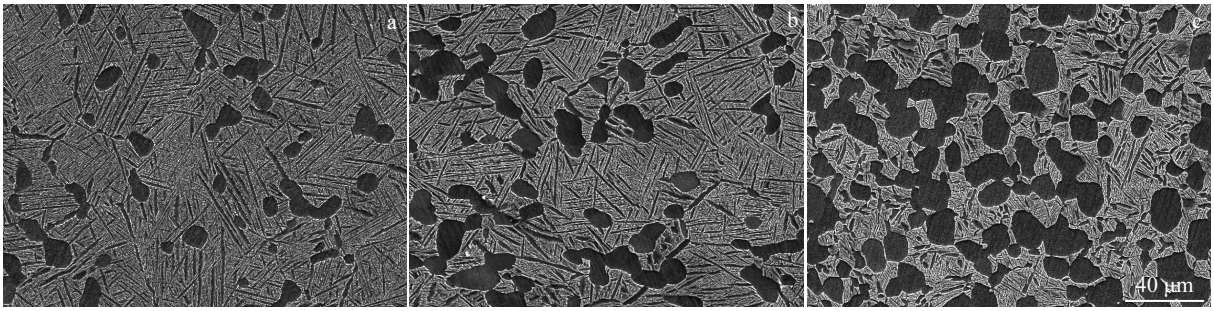

Fig.1 Microstructures of samples under different processing routes: (a) S12, (b) S22, and (c) S49

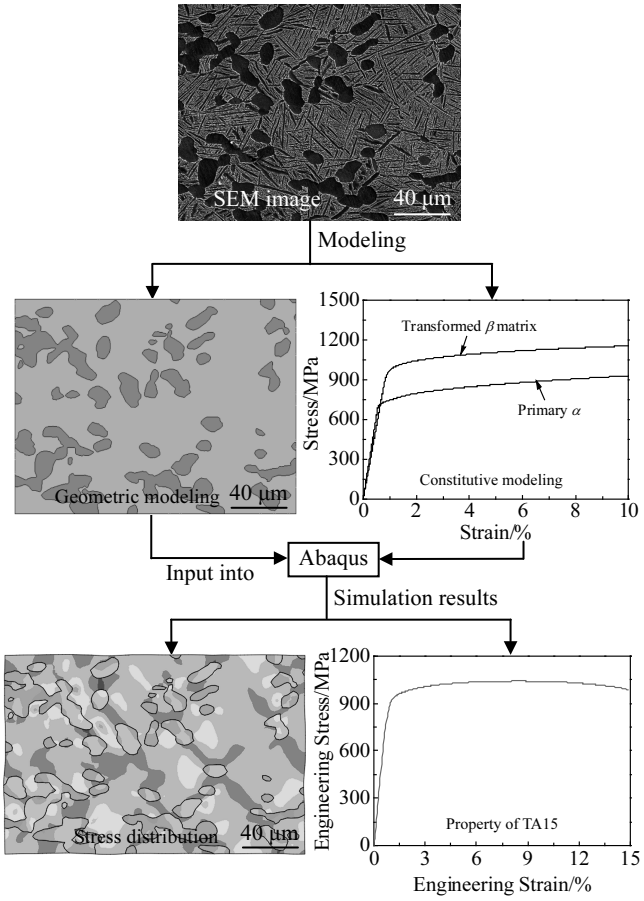

Fig.2 Procedure for microstructure-based finite element modeling

deformation of TA15 alloy were investigated. Fig.4 shows the distribution of equivalent stress in the RVEs with different volume fractions of α_p under UTS of the alloy. As shown in Fig.4a~4c, β_t generally undertakes larger stress than α_p. The distribution of microscopic stress is extremely complex in both α_p and β_t due to the inhomogeneous microstructure. Stress localized bands in β_t are distributed along the slant direction. α_p along the direction of β_t localized bands has relatively large stress due to large interaction between α_p and β_t. As the volume fraction of α_p increases, stress values in β_t decrease rapidly.

In order to have a more thorough understanding of the microstress, the stress histograms of α_p and β_t corresponding to Fig.4a~4c are given in Fig.4d~4f, respectively. As shown in Fig.4d~4f, the microstress in both α_p and β_t shows a normal

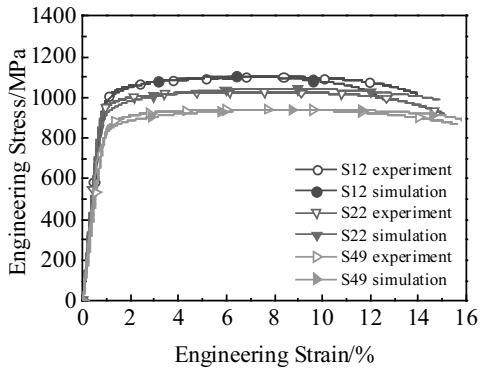

Fig.3 Predicted and experimental stress-strain curves

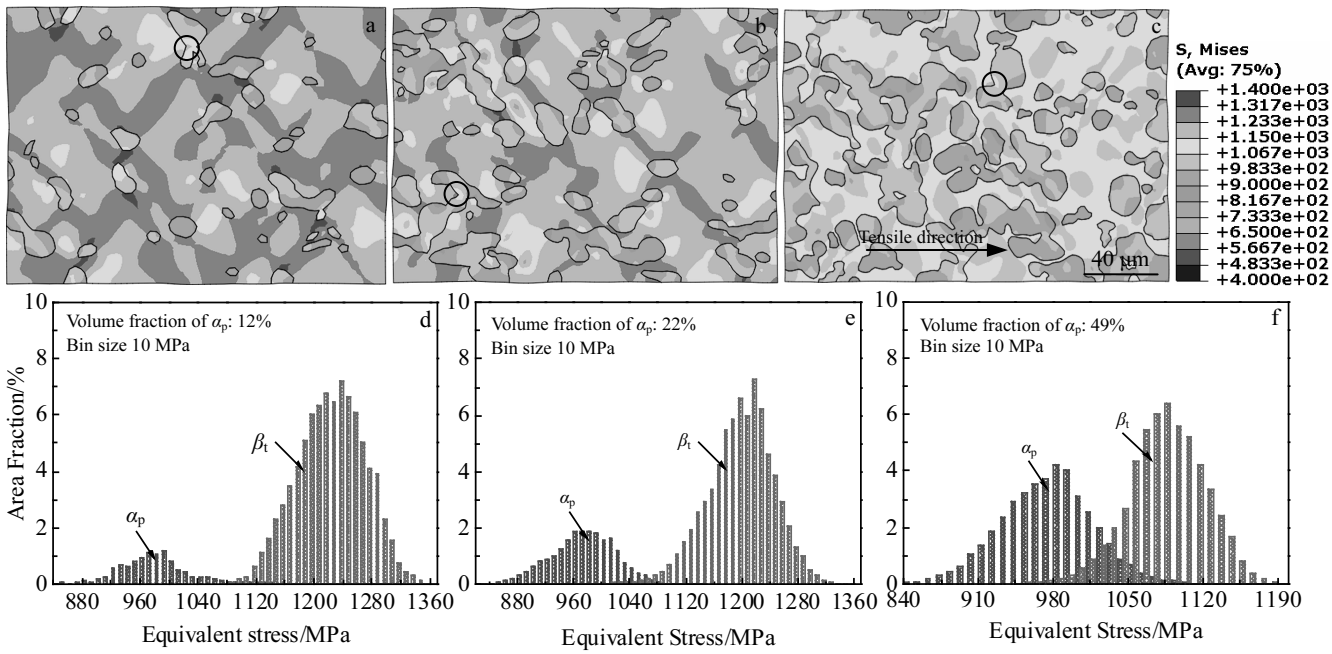

Fig.4 Distribution of equivalent stress (a~c) and corresponding stress histogram (d~f) of the RVEs under UTS condition with different α_p volume fractions: (a, d) 12%, (b, e) 22%, and (c, f) 49% (circles in Fig.4a~4c indicate the local high stress regions)

distribution with different peak heights and peak stresses. In the case of α_p, peak height increases from about 1.1% to 4.2% and peak stress varies slightly as the volume fraction of α_p increases. In the case of β_t, the peak height decreases slightly and the peak stress decreases from about 1240 MPa to 1080 MPa as the volume fraction of α_p increases. While, the peak height and peak stress of β_t are much larger than those of α_p. The larger peak height and peak stress indicate that more β_t undertakes larger load. Therefore, the results indicate that β_t contributes more to the UTS of the alloy.

The local stress has an important effect on the mechanical properties of titanium alloy. As shown in Fig.4, local high stress can be found at α side of α/β interfaces (indicated by circle in Fig.4a~4c). There are two reasons for local high stress. On the one hand, heterogeneity of the microstructure leads to the local stress during the deformation of titanium alloy. On the other hand, phase transformation can also lead to local stress. During formation process of microstructure, α_p may not keep Burgers OR with β phase[22,23]. Dislocations will pile up at α/β phase boundary and the dislocation density increases with the misorientation between two adjacent phases[24]. This dislocation was found in α_p and gathered along their boundary after heat treatment of titanium alloy [25]. The accumulation of dislocation causes transformation stress. This transformation stress combined with the deformation stress at the α_p boundary leads to void formation and failure of the alloy. Fig.4a~4c show that the local stress is more significant in the microstructure with lower α_p volume fraction. Therefore, failure strain of the alloy decreases with decreasing the volume fraction of α_p.

2.2 Microscopic strain distribution

Fig.5 shows the distribution of equivalent strain in the RVEs with different volume fractions of α_p under FS of the alloy. As shown in Fig.5a~5c, α_p undertakes larger strain than β_t. Strain localized bands in β_t always pass through α_p along slant direction. Comparing Fig.5a~5c and Fig.4a~4c, it can be found that the location of microscopic stress and strain localized bands is consistent since high stress regions are always high strain regions in each phase.

The strain histograms corresponding to Fig.5a~5c are displayed in Fig.5d~5f, respectively. As shown in Fig.5d~5f, with increasing the α_p volume fraction, peak height of α_p increases, whereas the peak strain decreases from about 0.21 to 0.15. In the case of β_t, the peak height decreases, while the peak strain slightly increases with increasing the α_p volume fraction. From Fig.5d~5f, it can also be seen that α_p has large peak strain, while β_t has large peak height. So, it is difficult to compare the contribution of α_p and β_t to the FS of the alloy.

2.3 Contribution of microscopic stress and strain to properties of TA15 alloy

The contribution of α_p and β_t to the UTS and FS of the alloy can be quantitatively evaluated by the ratio of average stress and strain between each constituent phase and RVEs, as defined below:

$$C_{i\mathrm{UTS}} = \sigma_i / \sigma_{\mathrm{R}} \quad (1)$$

$$C_{i\mathrm{FS}} = \varepsilon_i / \varepsilon_{\mathrm{R}} \quad (2)$$

where $C_{i\mathrm{UTS}}$ and $C_{i\mathrm{FS}}$ are the contribution of the i-th constituent phases to the UTS and FS of the alloy, respectively. Here, i-th constituent phase means α_p or β_t. σ_i and ε_i are the average stress and strain of the i-th constituent phases, respectively, which can be defined as:

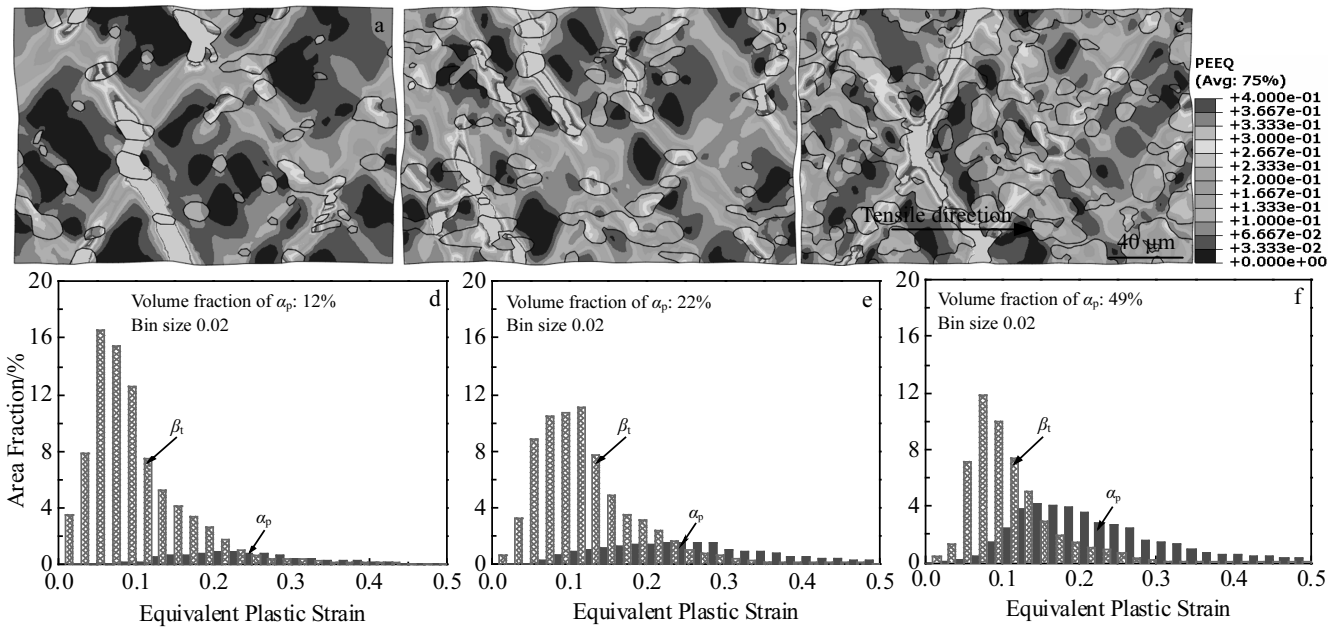

Fig.5 Distribution of equivalent strain (a~c) and corresponding strain histogram (d~f) of the RVEs under FS condition with different α_p volume fractions: (a, d) 12%, (b, e) 22%, and (c, f) 49%

$$\sigma_i = \sum_{w=1}^{n} \sigma_{iw} A_{iw} \quad (3)$$

$$\varepsilon_i = \sum_{w=1}^{n} \varepsilon_{iw} A_{iw} \quad (4)$$

where σ_{iw}, ε_{iw} and A_{iw} are the stress, strain and area fraction of w-th bin (Fig.4d~4f and Fig.5d~5f) in the i-th constituent phases, respectively. The average stress and strain of RVEs, σ_R and ε_R, can be simply obtained by:

$$\sigma_R = \sigma_{\alpha p} + \sigma_{\beta t} \quad (5)$$

$$\varepsilon_R = \varepsilon_{\alpha p} + \varepsilon_{\beta t} \quad (6)$$

where $\sigma_{\alpha p}$ and $\sigma_{\beta t}$ are the average stress of α_p and β_t, and $\varepsilon_{\alpha p}$ and $\varepsilon_{\beta t}$ are the average strain of α_p and β_t, respectively.

Fig.6 shows the calculated contribution of α_p and β_t to UTS and FS of the alloy. The calculated results for the RVEs with 33% and 43% α_p (not shown in this study for briefness) are included in Fig.6. As shown in Fig.6a, the contribution of α_p to UTS is always less than that of β_t to UTS. As the α_p volume fraction decreases from 49% to 12%, the contribution of β_t to UTS of the alloy increases from 59% to 91% and the contribution of α_p to UTS decreases from 41% to 9%. Fig.6 also shows the volume fraction of α_p and β_t at different heat treatment temperatures. Assuming that volume fraction is another indicator that represents the contributions of α_p and β_t and is named as volume contribution to be distinguished from the calculated stress and strain contribution. It can be seen from Fig.6a that the stress contribution is less than volume contribution for α_p and the situation for β_t is just opposite. The stress contribution couples the effect of various microstructural parameters, such as property, size, morphology and volume fraction. Therefore, the effect of these microstructural parameters makes the stress contribution different from the volume contribution. However, it can be seen from Fig.6a that these parameters lead to a small difference between stress contribution and volume contribution.

Fig.6b shows the contribution of α_p and β_t to FS of the alloy. As shown in Fig.6b, the contribution of β_t to FS of the alloy increases from 36% to 75% and the contribution of α_p to FS decreases from 64% to 25% as the α_p volume fraction decreases from 49% to 12%. At lower α_p volume fraction, the contribution of β_t to FS is even greater than that of α_p to FS. This is because the peak height of strain distribution of β_t is much higher than that of α_p (Fig.5d and 5e). Besides, it can be seen from Fig.6b that the strain contribution is much higher than volume contribution for α_p and the situation for β_t is also just opposite. This large difference which is also caused by various microstructural parameters indicates that FS is more sensitive to microstructural parameters than UTS.

It is of important engineering significance to simultaneously increase the strength and ductility of structural materials [26]. From above analysis, it can be seen that the contribution of α_p to UTS and FS simultaneously decreases and the contribution of β_t to UTS and FS concurrently increases as α_p volume

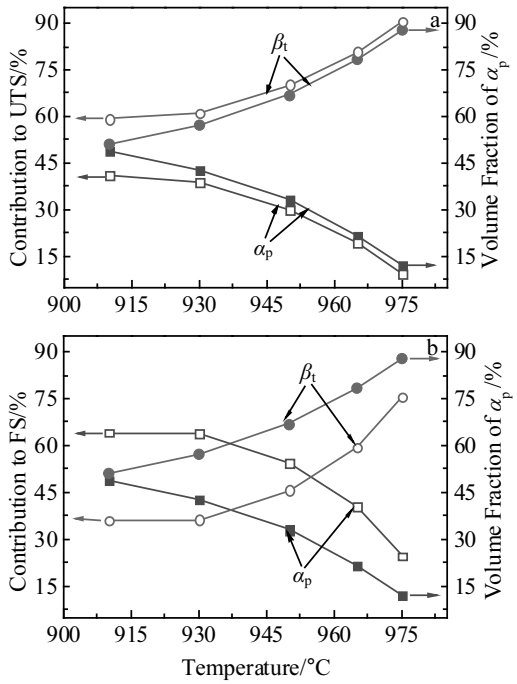

Fig.6 Contribution of the microstructural constituents to UTS (a) and FS (b) of TA15 alloy

fraction decreases. However, as α_p decreases from 49% to 12%, UTS of the alloy increases by 17% and FS decreases by 21% (UTS and FS are in Table 1). This means that it cannot concurrently increase UTS and FS of the alloy by increasing the contribution of β_t or decreasing contribution of α_p through decreasing α_p volume fraction. It should be noted here that the variation of α_p volume fraction involves the change of size and morphology of the constituent phases since it is difficult to only change α_p volume fraction and to remain other microstructural parameters unchanged in real microstructure. There are some other microstructural parameters, such as property and size that can be used to optimize the properties of the alloy. In these parameters, only increasing the strength of hard phase (i.e. β_t) cannot increase both the UTS and FS of the alloy, since increasing the strength of β_t can increase the UTS of alloy, but shifts the strain distribution of both α_p and β_t to low strain[27] and decreases the FS of the alloy. Increasing the strength of soft phase (i.e. α_p) may increase the UTS and FS at the same time, since increasing the strength of α_p can help to improve the UTS and concurrently lead to FS improvement because strain distribution of α_p and β_t may be more homogeneous. Besides, grain refinement is a generally used method to improve the UTS and FS of alloys[28]. Grain refinement can increase the uniformity of strain distribution in α_p and β_t and thus increase the FS of alloy[29]. Moreover, grain refinement is accompanied by an increase in strength due to Hall-Patch effect, therefore increasing the UTS of the alloy.

3 Conclusions

1) Microscopic stress in both α_p and β_t shows a normal distribution. The peak stress and stress peak height of β_t are much larger than those of α_p. While, α_p has large peak strain and β_t has large strain peak height.

2) As α_p volume fraction decreases from 49% to 12%, the contribution of β_t to UTS and FS increases from 59% to 91% and 36% to 75%, respectively. However, as the contribution of β_t increases, UTS of TA15 alloy increases by 17% and FS decreases by 21%.

3) This finding establishes an accurate correlation between constituent phases and mechanical properties of TA15 alloy, and gives a quantitative method to design the microstructure of titanium alloys.

References

1 Williams J C, Starke E A. *Acta Materialia*[J], 2003, 51(19): 5775

2 Fan X G, Yang H, Sun Z C *et al*. *Materials Science and Engineering A*[J], 2010, 527(21-22): 5391

3 Gao P F, Yang H, Fan X G *et al*. *Materials Science and Engineering A*[J], 2012, 540: 245

4 Wanjara P, Jahazi M, Monajati H *et al*. *Materials Science and Engineering A*[J], 2006, 416(1-2): 300

5 Tasan C C, Diehl M, Yan D *et al*. *Acta Materialia*[J], 2014, 81: 386

6 Stapleton A M, Raghunathan S L, Bantounas I *et al. Acta Materialia*[J], 2008, 56(20): 6186

7 Cho J R, Dye D, Conlon K T *et al*. *Acta Materialia*[J], 2002, 50(19): 4847

8 Hounkpati V, Fréour S, Gloaguen D *et al. Acta Materialia*[J], 2016, 109: 341

9 Kang J, Ososkov Y, Embury J D *et al. Scripta Materialia*[J], 2007, 56(11): 999

10 Lunt D, da Fonseca J Q, Rugg D *et al. Materials Science and Engineering A*[J], 2017, 680: 444

11 Koyama M, Yamanouchi K, Wang Q *et al. Materials Characterization*[J], 2017, 128: 217

12 Choi K S, Soulami A, Liu W N *et al. Computational Materials Science*[J], 2010, 50(2): 720

13 Sun X, Choi K S, Liu W N *et al. International Journal of Plasticity*[J], 2009, 25: 1888

14 Chan K S, Lee Y D. *Metallurgical and Materials Transactions A*[J], 2008, 39: 1665

15 Zhao X Q, Zang X L, Wamg Q F *et al. Rare Metals*[J], 2008, 27: 463

16 Srinivasu G, Rao R N, Nandy T K *et al. Materials and Design*[J], 2013, 46: 8

17 Ji Z, Yang H, Li H W. *Materials and Design*[J], 2015, 87: 171

18 Muszka K, Madej L, Wynne B P. *Archives of Civil and Mechanical Engineering*[J], 2016, 16: 224

19 Ji Z, Yang H, Li H W. *Materials Science and Engineering A*[J], 2015, 628: 358

20 Zhang X C, Zhong F, Shao J B *et al. Materials Science and Engineering A*[J], 2016, 676: 536

21 Sun X, Choi K S, Soulami A *et al. Materials Science and Engineering A*[J], 2009, 526(1-2): 140

22 Germain L, Gey N, Humbert M *et al*. *Acta Materialia*[J], 2008, 56: 4298

23 Gao P F, Cai Y, Zhan M *et al*. *Journal of Alloys and Compounds*[J], 2018, 741: 734

24 Zhu Y Y, Liu D, Tian X J *et al. Materials and Design*[J], 2014, 56: 445

25 Huang J, Wang Z R, Xue K M. *Materials Science and Engineering A*[J], 2011, 528(29-30): 8723

26 Wang Y M, Chen M W, Zhou F H *et al. Nature*[J], 2002, 419: 912

27 Ji Z, Yang H. *Materials Letters*[J], 2016, 184: 157

28 Calcagnotto M, Adachi Y, Ponge D *et al. Acta Materialia*[J], 2011, 59(2): 658

29 Ankem S, Margolin H. *Metallurgical and Materials Transactions A*[J], 1982, 13(4): 603

微观应力和应变对 Ti-6Al-2Zr-1Mo-1V 合金力学性能的影响分析

吉 喆，郭 涛，沈承金，徐 杰

(中国矿业大学，江苏 徐州 221116)

摘 要：分析组成相对钛合金力学性能的影响对组织设计极为重要。通过真实组织有限元模型分析了 α_p 和 β_t 中的应力和应变，并定量揭示了他们对 Ti-6Al-2Zr-1Mo-1V 钛合金强度和韧性的影响。结果表明，α_p 和 β_t 中的应力呈现正态分布。β_t 的峰值应力和应力峰高远大于 α_p。然而，α_p 具有较大的峰值应变，β_t 具有较大的应变峰高。随着 α_p 体积分数从 49%降低到 12%，β_t 对抗拉强度的贡献从 59%增加到 91%，对失效应变的贡献从 36%增加到 75%。然而，随着 β_t 贡献的增加，合金抗拉强度增加了 17%，失效应变降低了 21%。研究结果定量揭示了组成相对强度和韧性的贡献，为钛合金组织设计提供了基础。

关键词：微观应力和应变；组成相；力学性能；钛合金；有限元模拟

作者简介：吉 喆，男，1981 年生，博士，中国矿业大学材料学院，江苏 徐州 221116，电话：0516-83591879，E-mail: jizhe@cumt.edu.cn